








Structures and Properties of Known and Postulated Interstellar Cations

Lorenzo Tinacci^{1,2} , Stefano Pantaleone^{1,3} , Andrea Maranzana¹ , Nadia Balucani^{2,3,4} , Cecilia Ceccarelli² , and
Piero Ugliengo¹ 

¹Dipartimento di Chimica and Nanostructured Interfaces and Surfaces (NIS) Centre, Università degli Studi di Torino, via P. Giuria 7, I-10125 Torino, Italy
Lorenzo.Tinacci@univ-grenoble-alpes.fr

²Université Grenoble Alpes, CNRS, IPAG, F-38000 Grenoble, France

³Dipartimento di Chimica, Biologia e Biotecnologie, Università di Perugia, I-06123 Perugia, Italy

⁴Osservatorio Astrofisico di Arcetri, Largo E. Fermi 5, I-50125 Firenze, Italy

Received 2021 May 12; revised 2021 July 14; accepted 2021 July 18; published 2021 September 28

Abstract

Positive ions play a fundamental role in interstellar chemistry, especially in cold environments where chemistry is believed to be mainly ion driven. However, in contrast with neutral species, most of the cations present in the astrochemical reaction networks are not fully characterized in the astrochemical literature. To fill this gap, we have carried out new accurate quantum chemical calculations to identify the structures and energies of 262 cations with up to 14 atoms that are postulated to have a role in interstellar chemistry. Optimized structures and rotational constants were obtained at the M06-2X/cc-pVTZ level, while electric dipoles and total electronic energies were computed with CCSD(T)/aug-cc-pVTZ//M06-2X/cc-pVTZ single-point energy calculations. The present work complements the study by Woon & Herbst, who characterized the structure and energies of 200 neutral species also involved in interstellar chemistry. Taken together, the two data sets can be used to estimate whether a reaction, postulated in present astrochemical reaction networks, is feasible from a thermochemistry point of view and, consequently, to improve the reliability of the present networks used to simulate the interstellar chemistry. We provide an actual example of the potential use of the cations plus neutral data sets. It shows that two reactions, involving Si-bearing ions and present in the widely used reaction networks KIDA and UMIST, cannot occur in the cold interstellar medium because they are endothermic.

Unified Astronomy Thesaurus concepts: [Astrochemistry \(75\)](#); [Interstellar molecules \(849\)](#)

Supporting material: data behind figure, machine-readable table

1. Introduction

Soon after the first detection in the late 1960s of polyatomic molecules in interstellar cold (10–20 K) molecular clouds (Cheung et al. 1968, 1969; Snyder et al. 1969), the dominant role of cations in the chemistry leading to them became clear (Watson 1973; Herbst & Klemperer 1973). The reason is relatively simple: molecular clouds are too cold for reactions that present activation barriers to take place, and the vast majority of neutral–neutral reactions possess activation barriers (insurmountable at 10 K). Therefore, in cold molecular clouds, chemistry is believed to be mainly driven by cations, whose root is the ionization of hydrogen (both in the atomic and molecular forms) by the cosmic rays that permeate the Milky Way.

The first confirmation of this theoretical prediction came with the detection of HCO⁺ by Snyder et al. (1976).⁵ To date, out of slightly more than 200 interstellar detected species, about 30 are cations,⁶ the last ones discovered being HC₃S⁺ and CH₃CO⁺ (Cernicharo et al. 2021a, 2021b). Interestingly, all the 13 detected cations with more than three atoms are, so far, protonated forms of stable and abundant molecules. It is important to emphasize that the relatively low number of detected cations is not due to their real paucity, at least based on the astrochemical theoretical predictions, but on their low abundance and the difficulty of deriving their spectroscopic properties (e.g., McGuire et al. 2020).

As a matter of fact, of the about 500 species involved in the present astrochemical gas-phase reaction networks (e.g., KIDA⁷ and UMIST), more than half are cations. In the same vein, of the 8000 or so reactions in the same reaction networks, the majority, about 5500, involve cations. Yet, despite the obvious importance of cations in the modeling of interstellar chemistry, no systematic study exists in the literature on the structure and energy of the cations involved in these networks. Indeed, it is worth noting that the abovementioned reaction networks list cations whose structure has seldom been characterized and often appear as chemical formulae guessed on the basis of the reactions that involve them. In contrast, a systematic theoretical study of many neutral species present in the astrochemical reaction networks was carried out more than a decade ago by Woon & Herbst (2009).

The goal of the present work is to provide accurate physicochemical data for cation species, comparable in terms of methodology with those available for neutral species, to ultimately improve the accuracy of the astrochemical models. An obvious example of the impact of having reliable data of all species present in the astrochemical networks is that this will allow for quick verification of the exo-/endothermicity of the reaction, and, if relevant, excluding it from the network without the need for the very time-consuming characterization of the transition states of the reaction.

To reach the goal of providing reliable data on the cations, accurate estimates of the electronic spin multiplicity,

⁵ Actually, the theory followed the suggestion by Klemperer (1970) that an unidentified line observed in a few sources was to be attributed to HCO⁺.

⁶ <https://cdms.astro.uni-koeln.de/classic/molecules>

⁷ <http://kida.astrophy.u-bordeaux.fr/>

⁸ <http://udfa.ajmarkwick.net/>

geometrical structure, and absolute electronic energy of each cation are needed (Herzberg 1966; Lattelais et al. 2009, 2010; Chabot et al. 2013). Here we present new computations of the physicochemical properties of the 262 cations present in the KIDA astrochemical gas-phase reaction network (Wakelam et al. 2012).

The article is organized as follows. In Section 2, we provide details on the adopted computational methodology. In Section 3, we report the results of the new computations. In Section 4, we provide two examples of the possible application of the two data sets (the neutral one from Woon & Herbst (2009) and a cationic one from the present work) to identify and consequently exclude endothermic reactions present in the KIDA and UMIST reaction networks. Section 5 concludes the article and includes the hyperlink to the online database from this work, which is publicly available.

2. Methodology

2.1. Initial Guessed Geometrical Structures

In the astrochemical reaction networks, cations fall into two general classes of whether or not they are produced by ionization of a mother neutral species. Therefore, we adopted two different approaches to recover the initial guessed structures of the 262 cations.

For the 128 cations belonging to the first class (i.e., from ionization of a mother species), we started from the structure of the neutral species calculated by Woon & Herbst (2009), removing one electron and then optimizing the structure after assigning the proper charge and spin multiplicity. The reason behind this choice is that although cations are not produced by electron abstraction processes in most cases, astrochemical networks usually postulate that cation structures have the same connectivity of their neutral counterparts.

For about two-thirds of the remaining 134 cations, we retrieved the starting structures from the KIDA database⁷ and the NIST Computational Chemistry Comparison and Benchmark DataBase (CCCBDB).⁹ Finally, when only the brute formulas were available (about 50 cations), we guessed the starting structure case by case, looking at the products of the reactions forming and destroying the cations. To automatize the initial geometric guess for the unknown chemical structure, we developed a graph-theory-based software tool coupled with the Universal Force Field (Rappé et al. 1992) implemented in Rdkit (Landrum 2016). The script can be found in the online-only material and at the Astro-Chemistry Origin (ACO) Cations Scripts website.¹⁰

We emphasize that the procedures and choices described above stem from the fact that, very often, only simple connectivity or a cation name are available in the reaction networks and not the structure itself. In the few uncertain cases where *cis-trans* isomers are possible and no further information is available in the network to differentiate them, we assumed the most stable one (in the specific case, the *trans* isomer, based on the general rules of organic chemistry).

2.2. Computational Details

Once the 262 guessed geometrical structures were obtained, a sequence of geometric optimizations at the density functional theory (DFT) level were made, considering both electronic spin multiplicities in the ground and first excited states.

All calculations were carried out with the Gaussian16 program (Frisch et al. 2016). For the DFT calculations, we adopted the Minnesota method M06-2X (Zhao & Truhlar 2008) coupled with the triple- ζ Dunning's correlation consistent basis set (cc-pVTZ) (Kendall 1992; Woon & Dunning 1993) for geometry optimization. We kept the default values set up in Gaussian16 for: the DFT integration grid (i.e., 99,590 grid points), self-consistent field convergence (i.e., $\Delta E = 10^{-8}$ Ha on the rms density matrix and $\Delta E = 10^{-6}$ Ha on the maximum density matrix value and total energy), and geometry optimization tolerances (i.e., 3×10^{-4} Ha and 1.2×10^{-3} a₀, on rms gradients and displacements, respectively). We carefully explored symmetry constraints to maximize the number of symmetry elements compatible with the most stable structure. Harmonic frequency calculations were performed for all considered cases to ensure that each structure was a minimum of the potential energy surface (PES). Dipole moments and absolute electronic energies were refined at the coupled-cluster level with full single and double excitations and a perturbative treatment of triple excitations (CCSD(T) and ROCCSD(T); Knowles et al. 1993; Watts et al. 1993) in conjunction with an augmented triple- ζ correlation consistent basis set (aug-cc-pVTZ; Kendall 1992).

Since unrestricted electronic solutions are affected by spin contamination (i.e., the artificial mixing of different spin states) and this contribution is not negligible nor automatically corrected in Gaussian16 via the spin annihilation procedure, we adopted the Restricted Open (RO) formalism (except for singlet open, since the RO formalism is not applicable), whose wave function is the eigenfunction of the \hat{S}^2 operator, for all open shell configurations. Spin contamination causes problems in recovering dynamic correlation mainly in post-HF methods that are based on many-body perturbation theory (MP2, CCSD), because the perturbation through high-spin states is too large to be correctly accounted for by these methods (Watts et al. 1993).

Moreover, a stability analysis on the converged wave function was applied to the singlet states computed via the M06-2X/cc-pVTZ level (Bauernschmitt & Ahlrichs 1996) using the specific keywords (*opt = stable*) provided in Gaussian16 (see Figure 1; Ψ_{1c} stability block).

The scheme summarizing the adopted strategy is shown in Figure 1, where the various steps needed to reach the final minimum structure are shown.

Rendering of molecule images have been obtained via the VMD software (Humphrey et al. 1996), and the graphics elaboration and plots via the TikZ and PGFplots LATEX packages.

2.3. Benchmark Method

In order to test the accuracy of the above-described methodology, a benchmark on both structure and wave function optimizations using different methods was carried out.

Geometry optimization—We checked the M06-2X/cc-pVTZ level of theory by comparing our results obtained for a subset of molecules with those computed at the CCSD/aug-cc-pVTZ level, as shown in Table 1. Both the geometry rms deviation (RMSD) and the energy difference are small enough (less than ~ 0.045 Å

⁹ <http://cccbdb.nist.gov/>

¹⁰ aco-itn.oapd.inaf.it/aco-public-datasets/theoretical-chemistry-calculations/software-packages/cations-structures-scripts

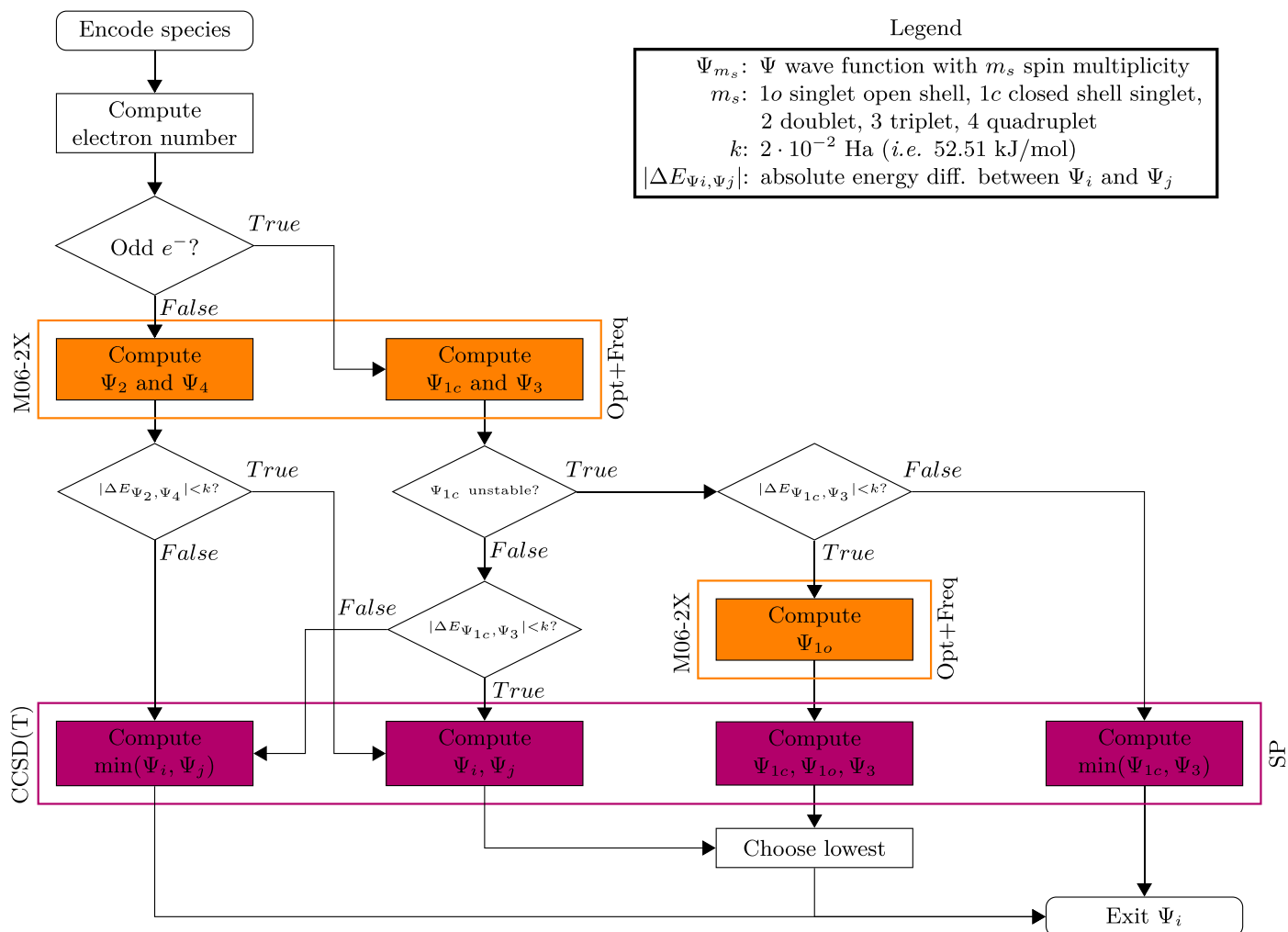


Figure 1. Adopted procedure to define the ground electronic state for a species and to achieve the related optimized geometry and cation properties. To this end, we used two levels of theory: M06-2X/cc-pVTZ and CCSD(T)/aug-cc-pVTZ. In the M06-2X block, a geometric optimization (Opt) and vibrational frequencies calculation (Freq) are performed to ensure that a minimum PES is achieved. In the CCSD(T) block, the final energy is then refined as a single-point evaluation at the CCSD(T) level together with the corresponding properties. The Ψ_{1c} stability is tested with the Gaussian16 wave function stability tool to find restricted \rightarrow unrestricted wave function instability.

and ~ 1.7 kJ mol $^{-1}$, respectively) to validate the present methodology. Moreover, the average ΔE is 0.522 kJ mol $^{-1}$, which is lower than the commonly accepted quantum mechanics calculation accuracy of ~ 4 kJ mol $^{-1}$ (i.e., 1 kcal mol $^{-1}$). The extended internal coordinates geometry optimization comparison is available in the [Appendix](#).

Wave function optimization—The procedure shown in Figure 1 was first tested on two very common molecules: ethylene (C₂H₆) and methylene (CH₂). These molecules present different ground states, i.e., singlet closed shell (1A_g) and triplet (3B_1) for ethylene and methylene, respectively. Their corresponding excited states are triplet (3A_1) for ethylene and singlet closed shell (1A_1) for methylene. Our calculated transition energies are in good agreement with the experimental data: 282 versus 272 kJ mol $^{-1}$ (Douglas et al. 1955) and 40 versus 38 kJ mol $^{-1}$ (Shavitt 1985) for ethylene and methylene, respectively. For the singlet closed shell methylene (1A_1) the stability analysis was also performed revealing a preference for the unrestricted solution with respect to the restricted one, as expected.

Dipole moment evaluation—Woon & Herbst (2009) showed that the CCSD(T)/aug-cc-pVTZ electronic dipole for neutral species is in good agreement with the experimental data. We

Table 1
Rms Displacement (RMSD) of Atomic Positions and the Absolute Energy Difference

Species	State	ΔE [kJ mol $^{-1}$]	RMSD [Å]
C ₂ ⁺	$^4\Sigma_g$	0.247	0.003
NH ₄ ⁺	1A_1	-0.022	0.000
H ₂ CO ⁺	2B_2	0.247	0.007
PNH ₂ ⁺	2B_2	0.512	0.005
l-C ₃ H ₂ ⁺	$^2A'$	0.055	0.045
H ₃ CS ⁺	3A_1	0.509	0.012
c-C ₃ H ₃ ⁺	$^1A_1'$	0.714	0.004
C ₄ H ₃ ⁺	1A_1	1.681	0.008
CH ₃ CHOH ⁺	$^1A'$	0.432	0.006
H ₂ C ₃ O ⁺	2B_2	0.845	0.005

Note. Calculated at CCSD(T)/aug-cc-pVTZ//M06-2X/cc-pVTZ compared with calculations at CCSD(T)/aug-cc-pVTZ//CCSD/aug-cc-pVTZ.

expect a similar or better agreement for cations, in virtue of the more contracted nature of the electron density compared to the more diffuse one in neutral species.

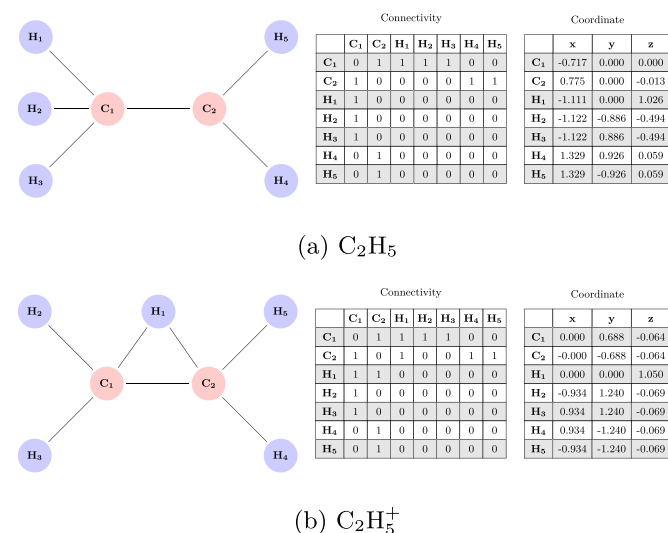


Figure 2. Graphs, connectivity matrices, and coordinates (in Å) of the neutral ethyl radical C_2H_5 and its cation $C_2H_5^+$.

2.4. Neutral versus Cation Structure Connectivity

Since many cation structures are derived from the neutral counterpart, we have calculated the ionization energy and followed the connectivity change (if any) after the geometry relaxation on the proper PES. In order to check if a cation retains the same connectivity of the neutral counterpart after geometric relaxation, the graph theory approach was used. Finally, the adiabatic ionization energy for the species that have a neutral counterpart will be presented in the dedicated subsection 3.2 with a comparison with available experimental data.

First, all the coordinate files are converted into chemical graphs (Trinajstić 2018) using the covalent radii and distance functions implemented in the Atomic Simulation Environment (ASE) python package (Larsen et al. 2017). A chemical graph is a nondirected graph where atoms and bonds in molecules correspond to nodes and edges, respectively. The different chemical elements present in the periodic table are represented in graphs as colors assigned to the vertices: the graph is, therefore, defined as a multicolored graph. Second, the graphs related to the neutral and ionized molecules are tested for isomorphism. Two graphs which contain the same number of colored vertices connected in the same way are considered isomorphic. The NetworkX python package (Hagberg et al. 2008) was used in order to deal with graph objects. Examples of chemical graphs are shown in Figure 2.

3. Results

The structures of the cations computed following the procedures and methodology described in the previous section are minima of PES when starting from the guessed ones, i.e., we did not explore the full PES in search of the global minimum. Indeed, our goal is to consider cations whose connectivity derives from the astrochemical reaction networks with structures based on the reactions giving rise to their formation. When more isomeric forms exist, we adopted the most stable one when specific information in the reaction network was missing. Finally, we cross-checked our computed cation structures with the literature ones, in the relatively few cases where they are available, and generally found a very good agreement.

Table 2
Predicted Equilibrium Structures and Properties of Diatomic Species

Species	State	Symmetry	μ	B_e	r_e	r_e (exp)
H_2^+	$2^1\Sigma_g$	$D_{\infty h}$	0.000	827.202	1.101	1.057 ^a
HeH^+	$1^1\Sigma$	$C_{\infty v}$	1.343	1010.927	0.788	
CH^+	$1^1\Sigma$	$C_{\infty v}$	1.565	428.701	1.126	1.131 ^b
NH^+	$2^2\Pi$	$C_{\infty v}$	1.834	466.167	1.074	
OH^+	$3^3\Sigma$	$C_{\infty v}$	2.127	501.498	1.031	1.029 ^a
HF^+	$2^2\Pi$	$C_{\infty v}$	2.478	518.136	1.010	
C_2^+	$4^4\Sigma_g$	$D_{\infty h}$	0.000	43.077	1.398	
CN^+	$1^1\Sigma$	$C_{\infty v}$	2.846	57.192	1.169	1.290 ^a
CO^+	$2^2\Sigma$	$C_{\infty v}$	3.286	60.629	1.103	
N_2^+	$2^2\Sigma_g$	$D_{\infty h}$	0.000	59.719	1.099	1.113 ^a
SiH^+	$1^1\Sigma$	$C_{\infty v}$	0.330	228.988	1.506	1.499 ^a
NO^+	$1^1\Sigma$	$C_{\infty v}$	0.603	61.361	1.050	1.062 ^a
CF^+	$1^1\Sigma$	$C_{\infty v}$	1.305	51.829	1.151	1.263 ^a
PH^+	$2^2\Pi$	$C_{\infty v}$	0.741	255.260	1.424	
O_2^+	$2^2\Pi_g$	$D_{\infty h}$	0.000	52.927	1.093	1.116 ^a
HS^+	$3^3\Sigma$	$C_{\infty v}$	1.170	278.193	1.364	
HCl^+	$2^2\Pi$	$C_{\infty v}$	1.634	295.614	1.321	
SiC^+	$4^4\Sigma$	$C_{\infty v}$	1.026	18.276	1.815	
SiN^+	$3^3\Pi$	$C_{\infty v}$	2.860	17.154	1.777	
CP^+	$3^3\Sigma$	$C_{\infty v}$	0.120	22.542	1.610	
CS^+	$2^2\Sigma$	$C_{\infty v}$	0.945	26.449	1.480	
PN^+	$2^2\Sigma$	$C_{\infty v}$	2.040	24.210	1.471	
NS^+	$1^1\Sigma$	$C_{\infty v}$	2.209	25.735	1.420	
PO^+	$1^1\Sigma$	$C_{\infty v}$	4.030	23.802	1.419	
SiF^+	$1^1\Sigma$	$C_{\infty v}$	3.599	18.802	1.541	
CCl^+	$1^1\Sigma$	$C_{\infty v}$	0.165	24.050	1.534	
SiO^+	$2^2\Sigma$	$C_{\infty v}$	3.253	21.372	1.524	
SO^+	$2^2\Pi$	$C_{\infty v}$	2.785	23.644	1.416	
ClO^+	$3^3\Sigma$	$C_{\infty v}$	0.569	21.249	1.472	
SiS^+	$2^2\Sigma$	$C_{\infty v}$	4.576	9.240	1.915	
S_2^+	$2^2\Pi_g$	$D_{\infty h}$	0.000	9.641	1.811	

Notes. μ is the electric dipole moment in Debye units. B_e is the rotational constant expressed in gigahertz referring to the equilibrium structure. r_e is the calculated internuclear equilibrium distance expressed in angstroms, meanwhile $r_e(\text{exp})$ are the available experimental data.

^a From Chase (1996).

^b From Huber (2013).

3.1. Cations Properties and Geometries

Tables 2–6 list the calculated properties of the 262 cations studied in this work. In the tables, we grouped the cations into five categories: (1) diatomic species (Table 2); (2) linear species with 3–12 atoms (Table 3); (3) C_{2v} symmetry species (Table 4); (4) planar species (excluding those belonging to point 3) (Table 5); (5) nonplanar species (Table 6). Within each table, cations are ordered by increasing number of atoms and, within each subset, by increasing molecular mass. A sample of the derived structures is shown in Figure 3.

Online-only material with extended information on all 262 cations is provided as data behind Figure 3. The center of the coordinate frame with respect to the dipole moment components is referred to is the center of nuclear charge. We also make the data publicly available on the website of the ACO project site.¹¹ The web-based ACO cation structure database¹² is based on the molecule hyperactive JSmol¹³ plugin. The ACO

¹¹ <https://aco-itn.oapd.inaf.it/home>

¹² aco-itn.oapd.inaf.it/aco-public-datasets/theoretical-chemistry-calculations/cations-database

¹³ JSmol is an open-source Java viewer for chemical structures in 3D (<http://www.jmol.org/>).

Table 3
Predicted Equilibrium Properties of Linear Polyatomic Species

Species	State	Symmetry	μ	B_e	Species	State	Symmetry	μ	B_e
C ₂ H ⁺	³ Π	C _{∞v}	0.755	41.665	SiC ₄ ⁺	² Σ	C _{∞v}	7.013	1.516
HCN ⁺	² Π	C _{∞v}	3.586	41.202	C ₄ P ⁺	¹ Σ	C _{∞v}	2.101	1.530
HNC ⁺	² Σ	C _{∞v}	0.148	47.950	C ₄ S ⁺	² Π	C _{∞v}	2.294	1.531
HCO ⁺	¹ Σ	C _{∞v}	4.172	45.359	C ₄ H ₂ ⁺	² Π _g	D _{∞h}	0.000	4.431
HOC ⁺	¹ Σ	C _{∞v}	2.380	44.893	HC ₂ NCH ⁺	¹ Σ	C _{∞v}	3.484	4.689
N ₂ H ⁺	¹ Σ	C _{∞v}	3.154	47.597	HC ₃ NH ⁺	¹ Σ	C _{∞v}	1.246	4.350
CNC ⁺	¹ Σ _g	D _{∞h}	0.000	13.661	C ₅ H ⁺	¹ Σ	C _{∞v}	2.677	2.420
C ₂ N ⁺	¹ Σ	C _{∞v}	2.660	12.004	HC ₄ N ⁺	² Π	C _{∞v}	6.436	2.327
CHSi ⁺	³ Σ	C _{∞v}	0.246	15.767	HC ₄ O ⁺	³ Σ	C _{∞v}	4.504	2.246
NCO ⁺	³ Σ	C _{∞v}	1.117	11.196	C ₆ ⁺	² Π _u	D _{∞h}	0.000	1.445
HNSi ⁺	² Σ	C _{∞v}	3.821	16.886	C ₅ N ⁺	³ Σ	C _{∞v}	3.890	1.391
HCP ⁺	² Π	C _{∞v}	0.985	18.914	SiC ₄ H ⁺	¹ Σ	C _{∞v}	2.487	1.440
CO ₂ ⁺	² Π _g	D _{∞h}	0.000	11.600	PC ₄ H ⁺	² Σ	C _{∞v}	0.274	1.444
HCS ⁺	¹ Σ	C _{∞v}	1.964	21.653	HC ₄ S ⁺	³ Σ	C _{∞v}	2.736	1.463
HSiO ⁺	¹ Σ	C _{∞v}	6.769	19.171	C ₆ H ⁺	³ Σ	C _{∞v}	3.410	1.393
HPN ⁺	¹ Σ	C _{∞v}	0.267	20.749	HC ₅ N ⁺	² Π	C _{∞v}	7.395	1.345
NO ₂ ⁺	¹ Σ _g	D _{∞h}	0.000	12.903	HC ₅ O ⁺	¹ Σ	C _{∞v}	2.586	1.308
SiC ₂ ⁺	² Σ	C _{∞v}	1.472	6.125	C ₇ ⁺	² Σ _u	D _{∞h}	0.000	0.912
SiNC ⁺	¹ Σ	C _{∞v}	4.015	6.653	C ₆ H ₂ ⁺	² Π _u	D _{∞h}	0.000	1.343
C ₂ S ⁺	² Π	C _{∞v}	1.112	6.489	H ₂ C ₅ N ⁺	¹ Σ	C _{∞v}	3.489	1.300
OCS ⁺	² Π	C _{∞v}	1.653	5.849	C ₇ H ⁺	¹ Σ	C _{∞v}	2.299	0.885
HSiS ⁺	¹ Σ	C _{∞v}	5.168	8.661	HC ₆ N ⁺	² Π	C _{∞v}	7.813	0.850
C ₂ H ₂ ⁺	² Π _u	D _{∞h}	0.000	33.595	C ₈ ⁺	² Σ _g	D _{∞h}	0.000	0.610
HCNH ⁺	¹ Σ	C _{∞v}	0.566	37.543	C ₇ N ⁺	³ Σ	C _{∞v}	4.860	0.587
C ₃ H ⁺	¹ Σ	C _{∞v}	2.552	11.262	C ₈ H ⁺	³ Σ	C _{∞v}	3.461	0.592
HSiNH ⁺	¹ Σ	C _{∞v}	3.460	17.494	HC ₇ N ⁺	² Π	C _{∞v}	8.764	0.570
C ₄ ⁺	² Π _g	D _{∞h}	0.000	4.836	HC ₇ O ⁺	¹ Σ	C _{∞v}	1.022	0.555
C ₃ O ⁺	² Σ	C _{∞v}	2.809	4.879	C ₉ ⁺	² Σ _u	C _{∞v}	0.011	0.429
C ₂ N ₂ ⁺	² Π _g	C _{∞v}	0.000	4.716	C ₈ N ⁺	¹ Σ	C _{∞v}	7.020	0.414
SiC ₂ H ⁺	¹ Σ	C _{∞v}	0.623	5.582	C ₈ H ₂ ⁺	² Π _g	D _{∞h}	0.000	0.574
PC ₂ H ⁺	² Π	C _{∞v}	0.219	5.803	C ₇ H ₂ N ⁺	¹ Σ	C _{∞v}	6.191	0.556
HC ₂ S ⁺	³ Σ	C _{∞v}	2.502	6.049	C ₉ H ⁺	¹ Σ	C _{∞v}	1.405	0.418
I-SiC ₃ ⁺	² Π	C _{∞v}	1.129	2.651	HC ₈ N ⁺	² Π	C _{∞v}	8.870	0.403
C ₃ S ⁺	² Σ	C _{∞v}	0.962	2.858	C ₁₀ ⁺	² Π _u	D _{∞h}	0.000	0.312
C ₄ H ⁺	³ Σ	C _{∞v}	3.140	4.640	C ₉ N ⁺	³ Σ	C _{∞v}	5.942	0.301
HC ₃ N ⁺	² Π	C _{∞v}	6.378	4.568	C ₁₀ H ⁺	³ Σ	C _{∞v}	3.258	0.304
HC ₃ O ⁺	¹ Σ	C _{∞v}	3.635	4.484	C ₉ HN ⁺	² Π	C _{∞v}	10.189	0.294
C ₅ ⁺	² Σ _u	D _{∞h}	0.000	2.596	HC ₉ O ⁺	¹ Σ	C _{∞v}	1.055	0.286
C ₄ N ⁺	¹ Σ	C _{∞v}	3.900	2.438	C ₁₁ ⁺	² Σ _u	D _{∞h}	0.000	0.235
SiC ₃ H ⁺	³ Σ	C _{∞v}	0.661	2.556	C ₁₀ N ⁺	¹ Σ	C _{∞v}	8.995	0.227
PC ₃ H ⁺	² Π	C _{∞v}	1.002	2.662	C ₁₀ H ₂ ⁺	² Π _u	D _{∞h}	0.000	0.296
HC ₃ S ⁺	¹ Σ	C _{∞v}	1.892	2.753	HC ₁₀ N ⁺	² Π	C _{∞v}	9.935	0.222

Note. μ is the electric dipole moment in Debye units. B_e is the rotational constant expressed in gigahertz referring to the equilibrium structure.

cation structure website will be periodically updated when new species will be added to the database. On the same site, we also provide the python script tool¹⁴ to convert molecules into a chemical graph and to exert control if two species share the same connectivity using the isomorphic function. The script can also be found in the online-only material.

Finally, while the rotational constants are reported in Tables 2 and 3 and in the web-based ACO cations database (for all the other nonlinear species), we warn the reader that the level of theory is not sufficiently accurate to allow their use for assigning bands in experimental spectra.

¹⁴ aco-itrn.oapd.inaf.it/aco-public-datasets/theoretical-chemistry-calculations/software-packages/cations-structures-scripts

3.2. Adiabatic Ionization Energy

Table 7 shows the adiabatic ionization energies (IE) for neutral species computed at CCSD(T)/aug-cc-pVTZ by Woon & Herbst (2009) along with those of the cation counterparts. All computed IE are without zero-point energy (ZPE) correction. Note that the cation counterparts are part of the group whose structures are derived from the ionization of neutral species, described in Section 2.1. As some of the data on larger molecules provided by Woon & Herbst (2009) are computed with a lower-quality basis set, we recomputed the energy for those species with the aug-cc-pVTZ.

The rms error between the computed ionization energies (adiabatic IE) and the experimental available data (vertical IE)

Table 4
Predicted Equilibrium Properties of Planar Polyatomic Species with C_{2v} Symmetry

Species	State	μ	Species	State	μ	Species	State	μ
CH_2^+	2A_1	0.488	H_2SiO^+	2B_2	3.737	$C_4H_3^+$	1A_1	0.297
NH_2^+	3B_1	0.559	PNH_2^+	2B_2	1.140	$PC_4H_2^+$	1A_1	3.268
H_2O^+	2B_1	2.201	H_2PO^+	1A_1	5.344	$C_5H_2^+$	2B_2	4.696
H_2F^+	1A_1	2.342	H_2CCl^+	1A_1	3.330	$H_2C_4N^+$	1A_1	8.037
NaH_2^+	1A_1	1.294	HSO_2^+	1A_1	3.802	$C_3H_5^+$	1A_1	0.815
SiH_2^+	2A_1	0.116	$H_2S_2^+$	2A_2	2.154	$C_5H_3^+$	1A_1	1.907
PH_2^+	1A_1	0.915	$C_2H_3^+$	1A_1	0.785	$CH_3OCH_3^+$	2B_1	0.791
H_2S^+	2B_1	1.466	$c-C_3H_2^+$	2A_1	1.128	$C_6H_3^+$	1A_1	1.721
C_3^+	2B_2	0.731	CH_2CN^+	1A_1	5.472	$C_7H_2^+$	2B_2	6.388
H_2Cl^+	1A_1	2.010	H_2CCN^+	1A_1	5.471	$H_2C_6N^+$	1A_1	10.568
SO_2^+	2A_1	1.871	H_2CCO^+	2B_1	3.539	$C_7H_3^+$	1A_1	3.426
CH_4^+	2B_2	1.478	$SiC_2H_2^+$	2B_2	0.038	$C_6H_5^+$	1A_1	1.330
H_2NC^+	1A_1	2.335	$PC_2H_2^+$	1A_1	1.973	$C_8H_3^+$	1A_1	3.505
H_2CO^+	2B_2	3.025	$CH_2NH_2^+$	1A_1	0.112	$C_9H_2^+$	2B_2	8.177
H_2NO^+	1A_1	3.639	$l-C_3H_3^+$	1A_1	0.727	$H_2C_8N^+$	1A_1	13.241
NaH_2O^+	1A_1	2.463	NH_2CNH^+	1A_1	0.180	$C_9H_3^+$	1A_1	5.329
CH_2Si^+	2A_1	2.280	$H_2C_3O^+$	2B_2	4.275	$C_9H_2N^+$	1A_1	13.766
PCH_2^+	1A_1	0.588	$SiC_3H_2^+$	2B_1	0.681	$C_{10}H_3^+$	1A_1	5.697
H_2CS^+	2B_2	2.013	$C_2H_5^+$	1A_1	0.612	$H_2C_{10}N^+$	1A_1	16.153

Note. μ is the electric dipole moment in Debye units.

Table 5
Predicted Equilibrium Properties of Planar Polyatomic Species without C_{2v} Symmetry

Species	State	Symmetry	μ	Species	State	Symmetry	μ
H_3^+	$^1A_1'$	D_{3h}	0.000	$HSiO_2^+$	$^1A'$	C_s	5.494
HNO^+	$^2A'$	C_s	2.908	H_2COH^+	$^1A'$	C_s	2.352
HO_2^+	3A	C_s	2.170	$l-C_3H_2^+$	$^2A'$	C_s	3.107
HNS^+	$^2A'$	C_s	1.439	$HCOOH^+$	$^2A'$	C_s	0.432
C_2O^+	2A	C_s	1.733	H_3SiO^+	$^1A'$	C_s	2.278
HPO^+	$^2A'$	C_s	2.962	PNH_3^+	$^1A'$	C_s	3.093
HSO^+	$^1A'$	C_s	3.336	$c-C_3H_3^+$	$^1A_1'$	D_{3h}	0.000
CCP^+	$^1A'$	C_s	2.381	$SiC_2H_3^+$	$^1A'$	C_s	0.224
HS_2^+	$^1A'$	C_s	1.496	$NH_2CH_2O^+$	$^1A'$	C_s	2.190
CH_3^+	$^1A_1'$	D_{3h}	0.000	$C_3H_3N^+$	$^2A''$	C_s	6.293
NH_3^+	$^2A_2''$	D_{3h}	0.000	$c-C_3H_2OH^+$	$^1A'$	C_s	2.492
SiH_3^+	$^1A_1'$	D_{3h}	0.000	$HCCCHOH^+$	$^1A'$	C_s	1.234
HC_2N^+	$^2A'$	C_s	5.002	$C_2H_3CO^+$	$^1A'$	C_s	2.743
C_2HO^+	$^1A'$	C_s	3.384	C_6N^+	$^1A'$	C_s	5.324
$HNCO^+$	$^2A''$	C_s	3.446	$C_4H_4^+$	$^2A''$	C_s	1.078
$HOCO^+$	$^1A'$	C_s	3.446	$C_3H_3NH^+$	$^1A'$	C_s	1.707
HN_2O^+	$^1A'$	C_s	3.706	$COOCH_4^+$	$^2A'$	C_s	3.196
C_3N^+	$^3A''$	C_s	2.921	$C_5H_5^+$	$^1A'$	C_s	1.219
$SiNCH^+$	$^2A'$	C_s	2.156	$C_6H_4^+$	2A_u	C_{2h}	0.000
$HOCS^+$	$^1A'$	C_s	2.274				

Note. μ is the electric dipole moment in Debye units.

is 0.308 eV. The difference between these two quantities is that in vertical IE (experimental) the geometry of the ionized molecule is not allowed to relax in its corresponding PES, while in adiabatic IE (computed) the energy of the ion is taken from the minimum of its PES. Therefore, adiabatic IE are expected to be always lower with respect to vertical IE, if calculated with the same methodology.

Connectivity change between neutral and cationic partners—Using the tools described in the Section 2.4, the atomic connectivity check was performed on the cations reported in

Table 7 and compared to the corresponding neutral species. The only cations that change their connectivity after the ionization and the subsequent geometric optimization are: C_3^+ , $C_2H_5^+$, and $C_4H_5^+$, as shown in Figure 4. For the C_3^+ this rearrangement explains the large difference (~ 1.4 eV) between our computed IE and the experimental vertical IE value.

This result corroborates our adopted methodology (Section 2), because it also demonstrates that the assumption in the astrochemical networks that many cations share the same connectivity as their neutral counterparts is respected.

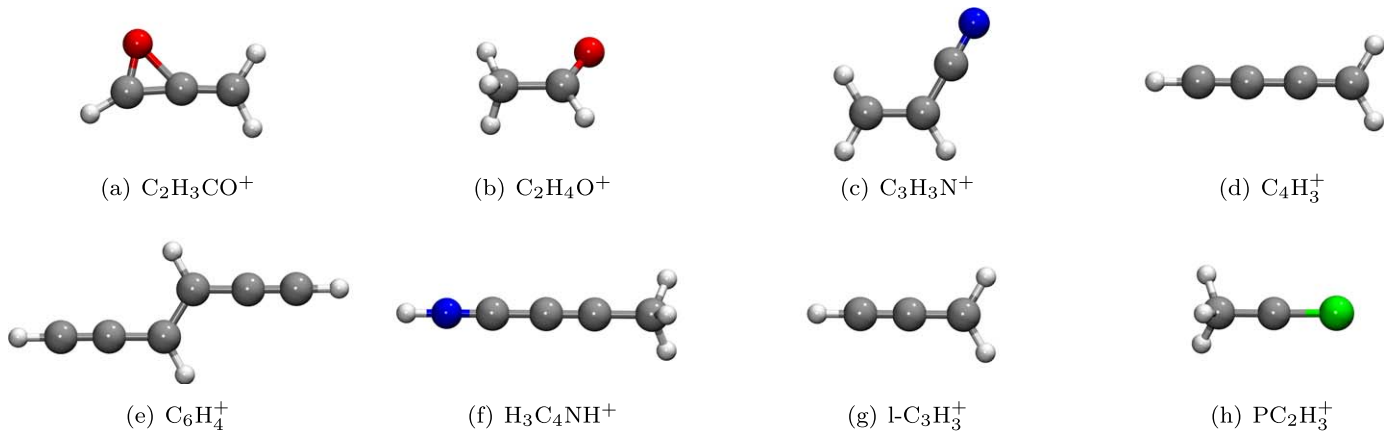


Figure 3. M06-2X/cc-pVTZ optimized structures of a sample of the cations studied in the present work. The structure of all the 262 cations is available online as data behind the figure and at the ACO Cations Database website (aco-itn.oapd.inaf.it/aco-public-datasets/theoretical-chemistry-calculations/cations-database).

(The data used to create this figure are available.)

Table 6
Predicted Equilibrium Properties of Nonplanar Polyatomic Species

Species	State	Symmetry	μ	Species	State	Symmetry	μ
H_3O^+	1A_1	C_{3v}	1.414	$CH_3NH_3^+$	1A_1	C_{3v}	2.166
PH_3^+	2A_1	C_{3v}	0.359	CH_3CHOH^+	$^1A'$	C_s	2.569
H_3S^+	1A_1	C_{3v}	1.554	$H_3C_4N^+$	$^2A'$	C_s	5.327
NH_4^+	1A_1	T_d	0.000	$C_2H_5OH^+$	2A	C_1	2.083
SiH_4^+	$^2A'$	C_s	1.222	$C_4H_5^+$	$^1A'$	C_s	0.860
$SiCH_3^+$	1A_1	C_{3v}	0.750	$H_5C_2O_2^+$	$^1A'$	C_s	0.972
H_3CS^+	3A_1	C_{3v}	0.559	$C_5H_4^+$	2B_3	D_2	0.000
PCH_3^+	$^2A''$	C_s	0.249	$H_3C_4NH^+$	1A_1	C_{3v}	2.635
$H_3S_2^+$	1A	C_1	2.292	$HCOCH_2OH_2^+$	$^1A'$	C_s	2.474
CH_5^+	$^1A'$	C_s	1.630	$C_5H_3N^+$	$^2A''$	C_s	6.270
$C_2H_4^+$	2B_3	D_2	0.000	$C_2H_5OH_2^+$	1A	C_1	3.312
CH_3OH^+	$^2A''$	C_s	1.394	$CH_3OCH_4^+$	$^1A'$	C_s	1.177
CH_3CO^+	1A_1	C_{3v}	2.977	$C_2H_6CO^+$	2B	C_2	1.567
SiH_5^+	$^1A'$	C_s	1.284	$C_5H_4N^+$	1A	C_1	5.401
$SiCH_4^+$	$^2A'$	C_s	1.224	$C_4H_7^+$	$^1A'$	C_s	1.480
PCH_4^+	$^3A''$	C_s	0.858	$C_3H_6OH^+$	1A	C_1	1.636
$PC_2H_3^+$	$^2A'$	C_s	0.375	$C_7H_4^+$	2B_2	D_2	0.000
$CH_3O_2^+$	1A	C_1	4.737	$H_3C_6NH^+$	1A_1	C_{3v}	4.646
CH_3CN^+	$^2A'$	C_s	2.604	$H_3C_7N^+$	2A	C_1	5.120
$CH_3NH_2^+$	$^2A'$	C_s	1.974	$C_7H_5^+$	$^1A'$	C_s	2.172
$CH_3OH_2^+$	$^1A'$	C_s	1.835	$C_8H_4^+$	2B_2	D_2	0.000
$C_3H_4^+$	2B_2	D_2	0.000	$C_6H_7^+$	$^1A'$	C_s	0.780
CH_3CNH^+	1A_1	C_{3v}	1.036	$C_8H_5^+$	$^1A'$	C_s	3.950
$C_2H_4O^+$	$^2A'$	C_s	2.056	$C_9H_4^+$	2A	C_1	0.391
$PC_2H_4^+$	$^1A'$	C_s	0.573	$C_8H_4N^+$	1A_1	C_{3v}	7.166
$C_2H_6^+$	2A_g	C_{2h}	0.000	$C_9H_5^+$	$^1A'$	C_s	3.960

Note. μ is the electric dipole moment in Debye units.

4. Discussion

As explained in the Introduction, having the physicochemical properties of the species involved in the astrochemical networks is a first basic step toward achieving accurate and reliable modeling. In this article, we complemented the work by Woon & Herbst (2009) on neutral species adding the physicochemical properties of the totality of cations present in the KIDA network⁷. In the following, we discuss a first, immediate application of the combined neutral plus cations

data sets: how the reaction energy, derived from the neutral and cations data sets, could be used to identify reactions that cannot happen in the conditions in the interstellar medium.

This example concerns two reactions, reported in Table 8, which involve SiS^+ . This cation has been postulated to be a precursor leading to SiS , a species observed in star-forming regions and associated with the molecular shocks of young forming protostars (Tercero et al. 2011; Podio et al. 2017). In

Table 7
Adiabatic Ionization Energy of the Corresponding Neutral Species

Species	eV	eV _(exp)	Species	eV	eV _(exp)	Species	eV	eV _(exp)	Species	eV	eV _(exp)
H ₂ ⁺	15.528	15.426 ^a	HNC ⁺	11.961	12.500 ^{ai}	C ₃ N ⁺	11.816		C ₆ H ⁺	9.336	
CH ⁺	10.562	10.640 ^b	HCO ⁺	8.037	8.140 ^{al}	C ₃ O ⁺	10.772		HC ₅ N ⁺	10.558	
NH ⁺	13.420	13.490 ^c	SiH ₂ ⁺	9.101		SiC ₂ H ⁺	7.289		C ₇ ⁺	10.293	
OH ⁺	12.899	13.017 ^d	HNO ⁺	10.165	10.100 ^{am}	C ₃ S ⁺	10.188		C ₆ N ⁺	8.866	
HF ⁺	15.998	15.980 ^e	PH ₂ ⁺	9.826	9.824 ^{an}	CH ₄ ⁺	12.749	12.610 ^{bh}	C ₂ H ₆ ⁺	11.619	11.570 ^{bw}
C ₂ ⁺	11.728	11.920 ^f	HO ₂ ⁺	11.306	11.350 ^{ao}	C ₂ H ₃ ⁺	8.678	8.250 ^{bi}	C ₃ H ₅ ⁺	8.029	
CN ⁺	13.715	14.170 ^b	H ₂ S ⁺	10.451	10.453 ^{ap}	SiH ₄ ⁺	11.050	11.200 ^{bl}	CH ₃ CHOH ⁺	6.662	
CO ⁺	13.959	14.014 ^g	C ₃ ⁺	11.606	11.610 ^{aq}	c-C ₃ H ₂ ⁺	9.118	9.150 ^{bm}	C ₅ H ₃ ⁺	8.124	
N ₂ ⁺	15.533	15.581 ^h	C ₂ N ⁺	10.730	12.000 ^{aq}	CH ₂ CN ⁺	10.211	10.300 ^{bn}	C ₆ H ₂ ⁺	9.477	
SiH ⁺	7.900	7.890 ⁱ	C ₂ O ⁺	10.912		H ₂ CCO ⁺	9.538	9.614 ^{bo}	C ₇ H ⁺	8.062	
NO ⁺	9.191	9.264 ^j	NCO ⁺	11.620	11.759 ^{ar}	SiCH ₃ ⁺	7.066		HC ₆ N ⁺	2.494	
PH ⁺	10.160	10.149 ^m	HNSi ⁺	11.718		HCOOH ⁺	11.282	11.310 ^{bp}	C ₈ ⁺	11.376	
O ₂ ⁺	12.053	12.070 ⁿ	HCP ⁺	10.786	10.790 ^{as}	C ₄ H ⁺	10.057		C ₇ N ⁺	9.659	
HS ⁺	10.310	10.421 ^o	CO ₂ ⁺	13.765	13.778 ^{at}	HC ₃ N ⁺	11.620		CH ₃ OCH ₃ ⁺	10.004	10.025 ^{bz}
HCl ⁺	12.716	12.790 ^p	HCS ⁺	7.588	7.412 ^{au}	C ₅ ⁺	11.116	12.300 ^{bq}	C ₄ H ₅ ⁺	7.066	
SiC ⁺	8.853	9.000 ^q	NO ₂ ⁺	9.458	9.600 ^{av}	C ₄ N ⁺	9.514		C ₈ H ⁺	8.836	
SiN ⁺	10.342		HPO ⁺	10.548		SiC ₃ H ⁺	8.181		HC ₇ N ⁺	9.825	
CP ⁺	10.914	10.500 ^r	SiNC ⁺	7.851		SiC ₄ ⁺	10.099		C ₉ ⁺	3.734	
CS ⁺	11.381	11.330 ^s	C ₂ S ⁺	10.186		C ₄ P ⁺	8.447		C ₈ N ⁺	8.430	
PN ⁺	11.933	11.880 ^t	OCS ⁺	11.189	11.185 ^{aw}	C ₄ S ⁺	9.199		C ₂ H ₆ CO ⁺	9.675	9.700 ^{ca}
NS ⁺	8.916	8.870 ^u	HSiS ⁺	8.260		C ₂ H ₄ ⁺	10.485	10.510 ^{br}	C ₅ H ₅ ⁺	7.718	
PO ⁺	8.476	8.390 ^v	SO ₂ ⁺	12.680	12.500 ^{az}	CH ₃ OH ⁺	10.928	10.850 ^{bs}	C ₆ H ₄ ⁺	8.993	
CCl ⁺	8.834	8.900 ^w	HS ₂ ⁺	9.376		CH ₃ CN ⁺	12.246	12.201 ^{bt}	C ₈ H ₂ ⁺	8.978	
SiO ⁺	11.521	11.300 ^z	CH ₃ ⁺	9.736	9.843 ^{ba}	C ₄ H ₂ ⁺	10.131		C ₉ H ⁺	7.742	
SO ⁺	10.428	10.294 ^{aa}	NH ₃ ⁺	10.148	10.020 ^{bb}	C ₅ H ⁺	8.358		HC ₈ N ⁺	8.387	
SiS ⁺	10.526	10.530 ^{ab}	C ₂ H ₂ ⁺	11.330	11.410 ^{bc}	HC ₄ N ⁺	9.425		C ₁₀ ⁺	10.647	
S ₂ ⁺	9.503	9.400 ^{ac}	H ₂ CO ⁺	10.900	10.880 ^{bd}	C ₆ ⁺	12.441		C ₉ N ⁺	9.168	
CH ₂ ⁺	10.338	10.350 ^{ad}	SiH ₃ ⁺	8.109	8.170 ^{be}	C ₅ N ⁺	10.705		C ₁₀ H ⁺	8.510	
NH ₂ ⁺	11.131	10.780 ^{ae}	HNCO ⁺	11.557	11.595 ^{bf}	SiC ₄ H ⁺	7.082		C ₁₁ ⁺	8.984	
H ₂ O ⁺	12.574	12.650 ^{af}	H ₂ CS ⁺	9.411	9.376 ^{bg}	C ₂ H ₅ ⁺	8.063	8.117 ^{bu}	C ₁₀ N ⁺	8.026	
C ₂ H ⁺	11.267	11.610 ^{ag}	H ₂ SiO ⁺	10.674		CH ₃ NH ₂ ⁺	9.061	8.900 ^{bv}	C ₁₀ H ₂ ⁺	8.722	
HCN ⁺	13.543	13.590 ^{ah}	C ₄ ⁺	10.734		C ₄ H ₃ ⁺	7.960		HC ₁₀ N ⁺	8.094	

Notes. Adiabatic ionization energy (eV) without ZPE correction, compared with the vertical experimental ionization energy (eV_(exp)).

^a (Shiner et al. 1993). ^b (Huber 2013). ^c (Dyke et al. 1980). ^d (Wiedmann et al. 1992). ^e (Tiedemann et al. 1979). ^f (Plessis & Marmet 1987). ^g (Erman et al. 1993). ^h (Trickl et al. 1989). ⁱ (Boo & Armentrout 1987). ^j (Reiser et al. 1988). ^k (Berkowitz & Cho 1989). ^l (Tonkyn et al. 1989). ^m (Milan et al. 1996). ⁿ (Wang et al. 1984). ^o (Verhaegen et al. 1964). ^p (Smoes et al. 1971). ^q (Drowart et al. 1978). ^r (Bulgin et al. 1977). ^s (Dyke et al. 1982). ^t (Hepburn et al. 1982). ^u (Nakasgawa et al. 1981). ^{aa} (Norwood & Ng 1989a). ^{ab} (Cockett et al. 1989). ^{ac} (Bender et al. 1988). ^{ad} (Reineke & Strein 1976). ^{ae} (Qi et al. 1995). ^{af} (Snow & Thomas 1990). ^{ag} (Norwood & Ng 1989b). ^{ah} (Dibeler & Liston 1968). ^{ai} (Bieri & Jonsson 1978). ^{aj} (Dyke 1987). ^{ak} (Lias et al. 1988). ^{al} (Tang et al. 2020). ^{am} (Walters & Blais 1984). ^{an} Rohlfling et al. (1984); only the upper limit value was reported. ^{ao} (Lias et al. 1988). ^{ap} (Dyke 1987). ^{aq} (Frost et al. 1973). ^{ar} (Wang et al. 1988). ^{as} (Ruscic & Berkowitz 1993). ^{at} (Clemmer & Armentrout 1992). ^{au} (Wang et al. 1988). ^{av} (Snow & Thomas 1990). ^{aw} (Berkowitz et al. 1994). ^{ax} (Qi et al. 1995). ^{ay} (Plessis & Marmet 1986). ^{az} (Ohno et al. 1995). ^{ba} (Nagano et al. 1993). ^{bb} (Ruscic & Berkowitz 1994). ^{bc} (Ruscic & Berkowitz 1993). ^{bd} (Berkowitz et al. 1994). ^{be} (Blush & Chen 1992). ^{bf} (Shin et al. 1990). ^{bg} (Clauberg et al. 1992). ^{bh} (Holmes et al. 1993). ^{bi} (Vogt et al. 1978). ^{bj} (Traeger 1985). ^{bk} (Ramanathan et al. 1993). ^{bl} (Ohno et al. 1995). ^{bm} (Tao et al. 1992). ^{bn} (Gochel-Dupuis et al. 1992). ^{bo} (Ruscic et al. 1989). ^{bp} (Aue & Bowers 1979). ^{bq} (Plessis & Marmet 1987). ^{br} (Butler et al. 1984). ^{bs} (Traeger et al. 1982).

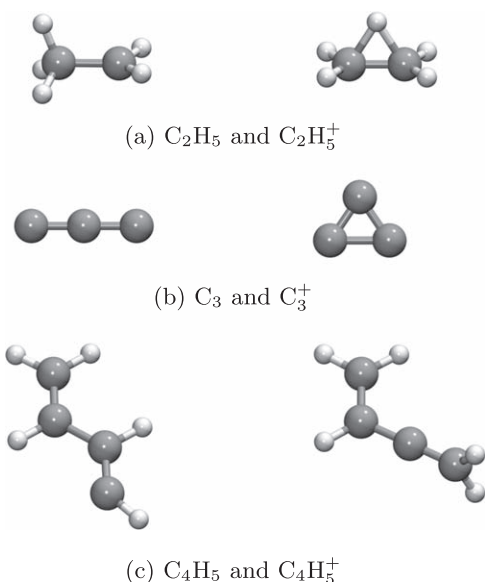
The calculated adiabatic ionization energies for C₄, C₆, C₈, and C₁₀ have been computed with respect to the triplet state of these species and not to the singlet state, as reported in Woon & Herbst (2009).

contrast to the competing S-bearing species SiO, which is likely extracted from the shattered grains, SiS is thought to be a product of gas-phase reactions (Podio et al. 2017). The KIDA database only lists one reaction forming SiS: HSiS⁺ + e → SiS + H. In turn, according to KIDA, HSiS⁺ is formed by the first reaction in Table 8: H₂ + SiS⁺ → H + HSiS⁺. Our computations, coupled with those by Woon & Herbst (2009), clearly show that this reaction is highly endothermic (~104 kJ mol⁻¹) and, consequently, rule out the formation of SiS by the recombination of HSiS⁺. Previous experimental work by Wlodek & Bohne (1989) support our conclusion. Therefore,

these two reactions (the formation of SiS from HSiS⁺) should be removed by the astrochemical reaction databases.

The second reaction in Table 8 involves the formation of SiS⁺, which would be the step before the above SiS reaction formation, according to the KIDA database (on the contrary, the UMIST database does not report the reaction). Also, in this case, our calculations show that the reaction is endothermic (~36 kJ mol⁻¹) and, therefore, should be removed from the database.

For the curious reader, other routes of SiS formation, involving neutral-neutral reactions, have been explored in the literature

**Figure 4.** Connectivity change between cations and the neutral species.**Table 8**

Two Examples of Endothermic Reactions Found in the Astrochemical Reaction Network for Molecular Clouds

Reaction	ΔE [kJ mol ⁻¹]
$H_2 + SiS^+ \rightarrow H + HSiS^+$	103.6
$SiS + S^+ \rightarrow SiS^+ + S$	36.1

Note. The reaction energy (i.e., ΔE , no ZPE correction) is computed with data from this work and Woon & Herbst (2009).

since the work of Podio et al. (2017) and found to be plausible (Rosi et al. 2018; Zanchet et al. 2018; Rosi et al. 2019).

5. Conclusions

In this work, we present new ab initio calculations of the structure and energy of 262 cations, all appearing in the used

astrochemical reaction network databases KIDA and UMIST. Our calculations complement the previous work by Woon & Herbst (2009), who reported the same properties for an ensemble of 200 neutral species. The rationale behind our new calculations is that accurate knowledge of the physico-chemical properties of the species in the reaction network databases is a first mandatory step to improving the reliability of the astrochemical models.

All the computed data can be found on the ACO project site.¹⁵

Finally, we discussed two practical examples to illustrate the potentiality of using our new cations database, coupled with the Woon & Herbst (2009) one, to identify and exclude endothermic reactions from the astrochemical reaction networks.

This project has received funding within the European Union’s Horizon 2020 research and innovation program from the European Research Council (ERC) for the project “The Dawn of Organic Chemistry” (DOC), grant agreement No. 741002, and from the Marie Skłodowska-Curie for the project “Astro-Chemical Origins” (ACO), grant agreement No. 811312. S.P., N.B., and P.U. acknowledge the Italian Space Agency for cofunding the Life in Space Project (ASI N. 2019-3-U.O). CINES-OCCIGEN HPC is kindly acknowledged for the generous allowance of supercomputing time through the A0060810797 project. Finally, we wish to acknowledge the extremely useful discussions with Professor Gretobape and the LATEX community for the insights on TikZ and PGFPlots packages.

Software: RdKit (Landrum 2016), ASE (Larsen et al. 2017), NetworkX (Hagberg et al. 2008), VMD (Humphrey et al. 1996), JSmol, Gaussian16 (Frisch et al. 2016).

Appendix

Extended Internal Coordinates Geometry Optimization Comparison

An extended internal coordinates geometry optimization comparison is provided in Table 9. The coordinates given in Table 9 follow those expressions in Gaussian16 for specifying generalized internal coordinates.¹⁶ The complete set of coordinate comparisons is available in a machine-readable format.

Table 9
Extended Internal Coordinates Geometry Optimization Comparison for $1-C_3H_2^+$

Species	Internal Z Vec.	Internal Coord.	M06-2X/cc-pVTZ	CCSD/aug-cc-pVTZ	Δ	Unit
$1-C_3H_2^+$	(1,6,6,6,1)	R(1,2)	1.093	1.092	0.001	Å
$1-C_3H_2^+$	(1,6,6,6,1)	R(2,3)	1.312	1.314	-0.002	Å
$1-C_3H_2^+$	(1,6,6,6,1)	R(2,5)	1.094	1.092	0.002	Å
$1-C_3H_2^+$	(1,6,6,6,1)	R(3,4)	1.340	1.351	-0.011	Å
$1-C_3H_2^+$	(1,6,6,6,1)	A(1,2,3)	120.665	120.424	0.241	Å
$1-C_3H_2^+$	(1,6,6,6,1)	A(1,2,5)	118.903	119.111	-0.208	Å
$1-C_3H_2^+$	(1,6,6,6,1)	A(3,2,5)	120.431	120.464	-0.032	Å
$1-C_3H_2^+$	(1,6,6,6,1)	L(2,3,4,5, -1)	172.977	179.999	-7.021	Å
$1-C_3H_2^+$	(1,6,6,6,1)	L(2,3,4,5, -2)	180.0	180.0	0	degrees
$1-C_3H_2^+$	(1,6,6,6,1)	D(1,2,5,3)	180.0	180.0	0	degrees

Note. Table 9 is published in its entirety in a machine-readable format. A portion is shown here for guidance regarding its form and content. (This table is available in its entirety in machine-readable form.)

¹⁵ aco-itn.oapd.inaf.it/aco-public-datasets/theoretical-chemistry-calculations/cations-database

¹⁶ Gaussian16 Revision C.01, <https://Gaussian.com/gic/>.

ORCID iDs

Lorenzo Tinacci  <https://orcid.org/0000-0001-9909-9570>
 Stefano Pantaleone  <https://orcid.org/0000-0002-2457-1065>
 Andrea Maranzana  <https://orcid.org/0000-0002-5524-8068>
 Nadia Balucani  <https://orcid.org/0000-0001-5121-5683>
 Cecilia Ceccarelli  <https://orcid.org/0000-0001-9664-6292>
 Piero Ugliengo  <https://orcid.org/0000-0001-8886-9832>

References

- Aue, D. H., & Bowers, M. T. 1979, *Gas Phase Ion Chemistry* (Amsterdam: Elsevier)
- Bauernschmitt, R., & Ahlrichs, R. 1996, *JChPh*, **104**, 9047
- Bender, H., Carnovale, F., Peel, J. B., & Wentrup, C. 1988, *JACHS*, **110**, 3458
- Berkowitz, J., & Cho, H. 1989, *JChPh*, **90**, 1
- Berkowitz, J., Ellison, G. B., & Gutman, D. 1994, *JPhCh*, **98**, 2744
- Berkowitz, J., Greene, J., Cho, H., & Ruscic, B. 1987, *JChPh*, **86**, 674
- Bieri, G., & Jonsson, B.-Ö. 1978, *CPL*, **56**, 446
- Blush, J. A., & Chen, P. 1992, *JPhCh*, **96**, 4138
- Boo, B. H., & Armentrout, P. 1987, *JACHS*, **109**, 3549
- Bulgín, D. K., Dyke, J. M., & Morris, A. 1977, *J. Chem. Soc., Faraday Trans.*, **73**, 983
- Butler, J. J., Holland, D. M., Parr, A. C., & Stockbauer, R. 1984, *IJMSI*, **58**, 1
- Cernicharo, J., Cabezas, C., Bailleux, S., et al. 2021b, *A&A*, **646**, L7
- Cernicharo, J., Cabezas, C., Endo, Y., et al. 2021a, *A&A*, **646**, L3
- Chabot, M., Béroff, K., Gratier, P., Jallat, A., & Wakelam, V. 2013, *ApJ*, **771**, 90
- Chase, M. W. 1996, *JPCRD*, **25**, 551
- Cheung, A., Rank, D. M., Townes, C., Thornton, D. D., & Welch, W. 1968, *PhRvL*, **21**, 1701
- Cheung, A., Rank, D. M., Townes, C., Thornton, D. D., & Welch, W. 1969, *Natur*, **221**, 626
- Clauberg, H., Minsek, D. W., & Chen, P. 1992, *JACHS*, **114**, 99
- Clemmer, D., & Armentrout, P. 1992, *JChPh*, **97**, 2451
- Cockett, M. C., Dyke, J. M., Morris, A., & Niavarán, M. H. Z. 1989, *J. Chem. Soc., Faraday Trans.*, **85**, 75
- Dibeler, V. H., & Liston, S. K. 1968, *JChPh*, **48**, 4765
- Douglas, J. E., Rabinovitch, B. t., & Looney, F. 1955, *JChPh*, **23**, 315
- Drowart, J., Smets, J., Reynaert, J., & Coppens, P. 1978, *Adv. Mass Spectrom.*, **7**, 647
- Dyke, J., Dunlavy, S., Jonathan, N., & Morris, A. 1980, *MolPh*, **39**, 1121
- Dyke, J. M. 1987, *J. Chem. Soc., Faraday Trans.*, **83**, 69
- Dyke, J. M., Morris, A., & Ridha, A. 1982, *J. Chem. Soc., Faraday Trans.*, **78**, 2077
- Dyke, J. M., Morris, A., & Trickle, I. R. 1977, *J. Chem. Soc., Faraday Trans.*, **73**, 147
- Ermann, P., Karawajczyk, A., Rachlew-Källne, E., et al. 1993, *CPL*, **215**, 173
- Frisch, M. J., Trucks, G. W., Schlegel, H. B., et al. 2016, *Gaussian Revision B.01* (Wallingford, CT: Gaussian, Inc.)
- Frost, D., Lee, S., & McDowell, C. 1973, *CPL*, **23**, 472
- Gochel-Dupuis, M., Delwiche, J., Hubin-Franskin, M.-J., & Collin, J. 1992, *CPL*, **193**, 41
- Hagberg, A. A., Schult, D. A., & Swart, P. J. 2008, *Proc. 7th Python in Science Conf.*, ed. G. Varoquaux, T. Vaught, & J. Millman, **11**, http://conference.scipy.org/proceedings/scipy2008/paper_2/
- Hepburn, J., Trevor, D., Pollard, J., Shirley, D., & Lee, Y. 1982, *JChPh*, **76**, 4287
- Herbst, E., & Klemperer, W. 1973, *ApJ*, **185**, 505
- Herzberg, G. 1966, *Electronic Spectra and Electronic Structure of Polyatomic Molecules*, Vol. 3 (New York: Van Nostrand)
- Holmes, J., Lossing, F., & Mayer, P. 1993, *CPL*, **212**, 134
- Huber, K.-P. 2013, *Molecular Spectra and Molecular Structure: IV. Constants of Diatomic Molecules* (Berlin: Springer Science & Business Media)
- Humphrey, W., Dalke, A., & Schulten, K. 1996, *J. Mol. Graph.*, **14**, 33
- Kendall, T., Jr 1992, *JChPh*, **96**, 6796
- Klemperer, W. 1970, *Natur*, **227**, 1230
- Knowles, P. J., Hampel, C., & Werner, H.-J. 1993, *JChPh*, **99**, 5219
- Landrum, G. 2016, *RDKit: Open-Source Cheminformatics Software*, <https://www.rdkit.org/>
- Larsen, A. H., Mortensen, J. J., Blomqvist, J., et al. 2017, *JPCM*, **29**, 273002
- Lattalais, M., Puzat, F., Ellinger, Y., & Ceccarelli, C. 2009, *ApJL*, **696**, L133
- Lattalais, M., Puzat, F., Ellinger, Y., & Ceccarelli, C. 2010, *A&A*, **519**, A30
- Lias, S. G., Bartmess, J. E., Liebman, J., Holmes, J., & Levin, R. D. 1988, *JPCRD*, **17**, Suppl. 1, <https://srdr.nist.gov/JPCRD/jpcrdSIVol17.pdf>
- McGuire, B. A., Asvany, O., Brünken, S., & Schlemmer, S. 2020, *NatRP*, **2**, 402
- Milan, J., Buma, W., & De Lange, C. 1996, *JChPh*, **104**, 521
- Nagano, Y., Murthy, S., & Beauchamp, J. 1993, *JACHS*, **115**, 10805
- Nakasgawa, H., Asano, M., & Kubo, K. 1981, *JNuM*, **102**, 292
- Norwood, K., & Ng, C. 1989a, *CPL*, **156**, 145
- Norwood, K., & Ng, C. 1989b, *JChPh*, **91**, 2898
- Ohno, K., Okamura, K., Yamakado, H., et al. 1995, *JPhCh*, **99**, 14247
- Plessis, P., & Marmet, P. 1986, *IJMSI*, **70**, 23
- Plessis, P., & Marmet, P. 1987, *CaCh*, **65**, 2004
- Podio, L., Codella, C., Lefloch, B., et al. 2017, *MNRAS*, **470**, L16
- Qi, F., Sheng, L., Zhang, Y., Yu, S., & Li, W.-K. 1995, *CPL*, **234**, 450
- Ramanathan, R., Zimmerman, J. A., & Eyley, J. R. 1993, *JChPh*, **98**, 7838
- Rappé, A. K., Casewit, C. J., Colwell, K., Goddard, W. A., III, & Skiff, W. M. 1992, *JACHS*, **114**, 10024
- Reineke, W., & Strein, K. 1976, *Berichte der Bunsengesellschaft für physikalische Chemie*, **80**, 343
- Reiser, G., Habenicht, W., Müller-Dethlefs, K., & Schlag, E. W. 1988, *CPL*, **152**, 119
- Rohlfing, E. A., Cox, D. M., & Kaldor, A. 1984, *JChPh*, **81**, 3322
- Rosi, M., Mancini, L., Skouteris, D., et al. 2018, *CPL*, **695**, 87
- Rosi, M., Skouteris, D., Balucani, N., et al. 2019, *International Conference on Computational Science and Its Applications* (Berlin: Springer), 306
- Ruscic, B., & Berkowitz, J. 1993, *JChPh*, **98**, 2568
- Ruscic, B., & Berkowitz, J. 1994, *JChPh*, **100**, 4498
- Ruscic, B., Berkowitz, J., Curtiss, L., & Pople, J. 1989, *JChPh*, **91**, 114
- Shavitt, I. 1985, *Tetrahedron*, **41**, 1531
- Shin, S. K., Corderman, R. R., & Beauchamp, J. 1990, *IJMSI*, **101**, 257
- Shiner, D., Gilligan, J., Cook, B., & Lichten, W. 1993, *PhRvA*, **47**, 4042
- Smoes, S., Myers, C., & Drowart, J. 1971, *CPL*, **8**, 10
- Snow, K. B., & Thomas, T. F. 1990, *IJMSI*, **96**, 49
- Snyder, L., Le, S., & Jm, H. 1976, *Reprints: Series A*, Vol. 212 (Green Bank, WV: National Radio Astronomy Observatory), 383
- Snyder, L. E., Buhl, D., Zuckerman, B., & Palmer, P. 1969, *PhRvL*, **22**, 679
- Tang, X., Lin, X., Garcia, G. A., et al. 2020, *JChPh*, **153**, 124306
- Tao, W., Klemm, R., Nesbitt, F., & Stief, L. 1992, *JPhCh*, **96**, 104
- Tercero, B., Vincent, L., Cernicharo, J., Viti, S., & Marcelino, N. 2011, *A&A*, **528**, A26
- Tiedemann, P., Anderson, S., Ceyer, S., et al. 1979, *JChPh*, **71**, 605
- Tonkyn, R. G., Winniczek, J. W., & White, M. G. 1989, *CPL*, **164**, 137
- Traeger, J. C. 1985, *IJMSI*, **66**, 271
- Traeger, J. C., McLoughlin, R. G., & Nicholson, A. 1982, *JACHS*, **104**, 5318
- Trickl, T., Cromwell, E., Lee, Y., & Kung, A. 1989, *JChPh*, **91**, 6006
- Trinajstić, N. 2018, *Chemical Graph Theory* (London: Routledge)
- Verhaegen, G., Stafford, F., & Drowart, J. 1964, *JChPh*, **40**, 1622
- Vogt, J., Williamson, A. D., & Beauchamp, J. 1978, *JACHS*, **100**, 3478
- Wakelam, V., Herbst, E., Loison, J.-C., et al. 2012, *ApJS*, **199**, 21
- Walters, E., & Blais, N. C. 1984, *JChPh*, **80**, 3501
- Wang, L.-S., Reutt, J., Lee, Y., & Shirley, D. 1988, *JESRP*, **47**, 167
- Wang, R.-G., Dillon, M., & Spence, D. 1984, *JChPh*, **80**, 63
- Watson, W. D. 1973, *ApJL*, **183**, L17
- Watts, J. D., Gauss, J., & Bartlett, R. J. 1993, *JChPh*, **98**, 8718
- Wiedmann, R., Tonkyn, R., White, M., Wang, K., & McKoy, V. 1992, *JChPh*, **97**, 768
- Wlodek, S., & Bohme, D. K. 1989, *J. Chem. Soc., Faraday Trans.*, **85**, 1643
- Woon, D. E., & Dunning, T. H., Jr 1993, *JChPh*, **98**, 1358
- Woon, D. E., & Herbst, E. 2009, *ApJS*, **185**, 273
- Zanchet, A., Roncero, O., Agúndez, M., & Cernicharo, J. 2018, *ApJ*, **862**, 38
- Zhao, Y., & Truhlar, D. G. 2008, *Theor. Chem. Acc.*, **120**, 215